Photorefractive properties of liquid crystal-filled bacterial cellulose mats

By

Caroline Novak
Department of Physics, Case Western Reserve University
cmn34@case.edu

Advisor
Dr. Kenneth Singer
Department of Physics, Case Western Reserve University
kds4@case.edu

December 17, 2017

Table of Contents

1. Executive Summary

The photorefractive effect is a phenomenon associated with nonlinear optical materials in which the refractive index of the material varies with the application of light. One demonstration of this effect is dynamic holography. Energy transfer between diffracted beams can be used, for example, to determine the properties of the sample under investigation, such as the coupling coefficient. It has been found that the strong photorefractive effect in liquid crystal cells arises from photoinduced surface charge modulation on the transparent conducting surface [1]. This limits the photorefractive holograms to the thin film regime, which is of limited use for dynamic holography applications. Bacterial cellulose (BC) mats, made easily by fermentation, can provide a complex nanoscale network of cellulose fibers that can be infiltrated with liquid crystals. Properly treated fiber surfaces could provide a dense network of photosensitive surfaces that would permit the generation of thick film gratings for dynamic holography, while providing for the robust photorefractive response of liquid crystals. In this project, I use dynamic holography techniques to explore the photorefraction of nematic liquid crystal-infiltrated BC mats.

2. Introduction

Organic electronics is a growing field that deals with devices made from conductive polymers. When compared to inorganic electronics, organic electronics provide a green alternative with additional benefits: organic electronics are lighter, more flexible, cheaper to manufacture, and less toxic [2]. Their biodegradability is also an attractive quality in some cases. Some potential applications of these devices include soft electronics, biological interfacing, optoelectronic devices, and more. Optoelectronics make up the broad field of electronic devices that involve light. This includes solar cells, photomultipliers, light-emitting diodes (LEDs), and liquid crystal displays. As the efficiency of organic devices improve, it is important to explore the properties and uses of these organic systems in order to stay on the forefront of innovation.

The electro-optic effect is the change in a material's optical properties due to an electric field. The combination of the electro-optic effect and photoconductivity results in the photorefractive effect. This project will explore the photorefractive properties of BC mats infiltrated with a nematic liquid crystal. The photorefractive effect can be utilized in a number of applications, such as image processing, optical switching, phase conjugation, optical limiting, optical computing, and simulations of neural networks [3,4]. However, this project will focus on the application of the photorefractive effect in dynamic holography.

3. Background

3.1. Photorefractive Effect

The photorefractive effect is the modulation of the refractive index in photoconductive materials when light is applied. A pictorial representation of the involved mechanisms for this effect is outlined in Figure 1. Two incident beams of light, when mixed within the material, create a diffraction grating, or a pattern of alternating light and dark regions. Since the material is photoconductive, charge carriers are generated in the regions of high intensity light. The mobile charges then migrate either by diffusion due to charge density gradients, or by drift with the application of an external electric field and

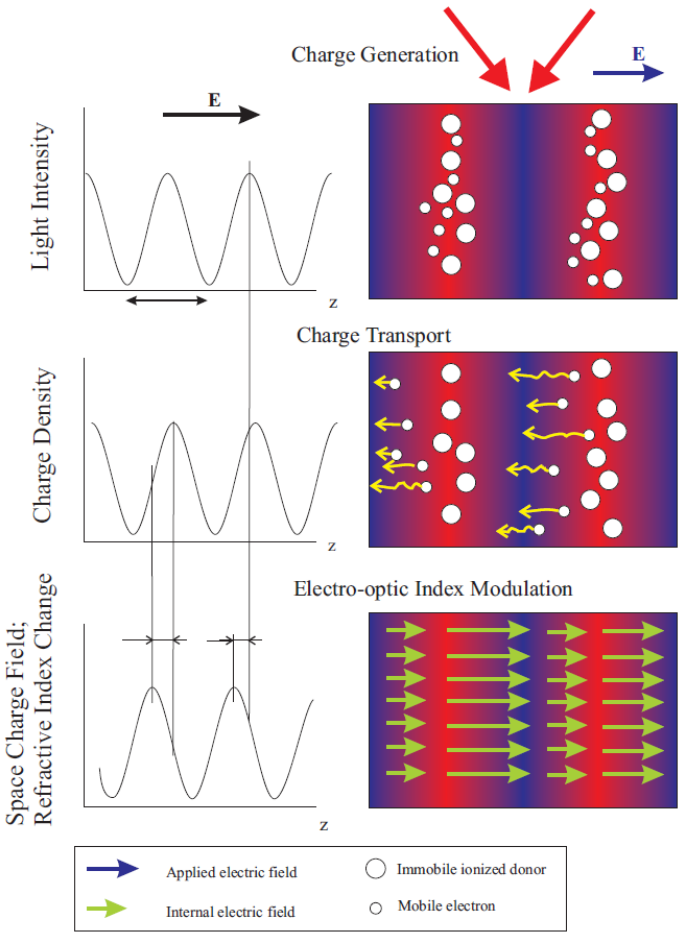

Figure 1: Photorefractive grating formation. From top to bottom: charge photogeneration, charge transport, and refractive index modulation [4]

eventually get trapped. This results in a sinusoidal space charge electric field, which induces a spatial modulation of the refractive index [4].

In the case of photorefractive materials, the refractive index grating that is induced by the mechanism described above is the hologram. This holographic grating can persist as long as it is illuminated by the two beams. When not illuminated, the grating will decay with a characteristic time constant. In addition, it can be easily erased by flooding the material with a uniform beam of light to redistribute the electrons in a more uniform manor [5,6]. This makes photorefractive materials ideal for dynamic holography and reusable optical storage.

3.2. Liquid Crystal

Liquid crystals are a popular material for studying the photorefractive effect due to their large orientational response. Liquid crystal is a phase of matter in which

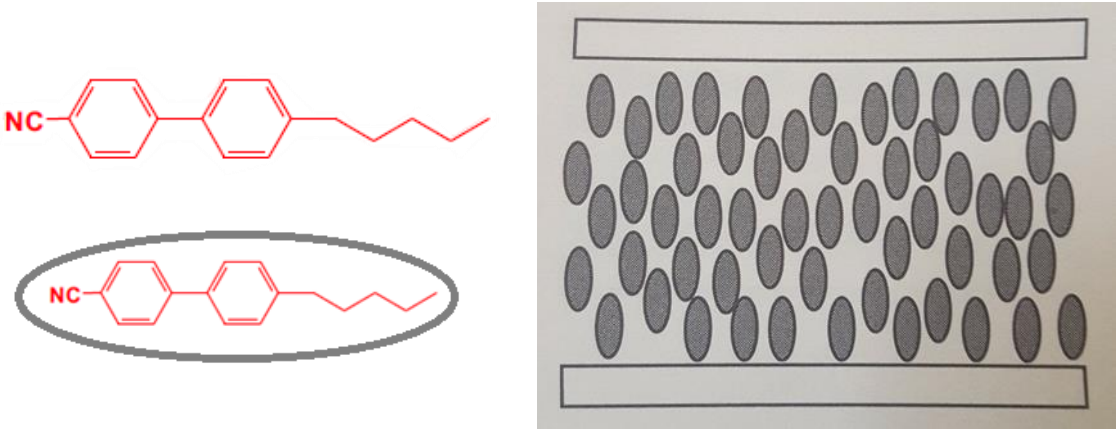

Figure 2: Molecular structure of 5CB (top left) [4], 5CB approximated by elongated ovals (bottom left), and the 5CB homeotropically aligned nematic phase structure (right) [7].

the material is fluid and lacking positional order, but there is some orientational order. The nematic liquid crystal phase is characterized by rod-like molecules aligning with their long axes approximately parallel in a direction represented by the director [7]. The mesogen, 4-cyano-4'-pentylbiphenyl (5CB) will be the material used in this project because it is a well-studied liquid crystal that is in the nematic phase at room temperature. A sandwich cell configuration (see Section 5.2) can be easily filled with 5CB because it is a small molecule with a low viscosity. Additionally, 5CB's hydrophobic hydrocarbon tail, hydrophilic end, and dipole moment allow it to be easily aligned to surfaces and reoriented with the application of an electric field [8].

Previous studies [7,9] have found that the photorefractive effect in cells of homeotropically aligned nematic liquid crystals are mediated by surface charge rather than bulk currents. This means that the refractive index grating is confined near to the liquid crystal-cell interface, limiting the usable wave vectors (crossing angles) effect to thin films, which is of limited use to dynamic holography due to the appearance of multiple diffraction orders.

3.3. Bacterial Cellulose

Bacterial cellulose (BC) is an organic material that is grown through fermentation. The final product is a unique nano-porous network of cellulose fibers with interesting properties, such as high crystallinity, water holding capability, high porosity, and biodegradability and biocompatibility [10]. There are also many functional groups on its surface, as seen in Figure 3, that facilitate the tailoring of its chemical and physical properties. By combining the photorefractive properties of 5CB and the unique structure of BC mats, it may be possible to expand the photorefractive effect to the thick film region via the dense network of 5CB-BC volume-distributed interfaces.

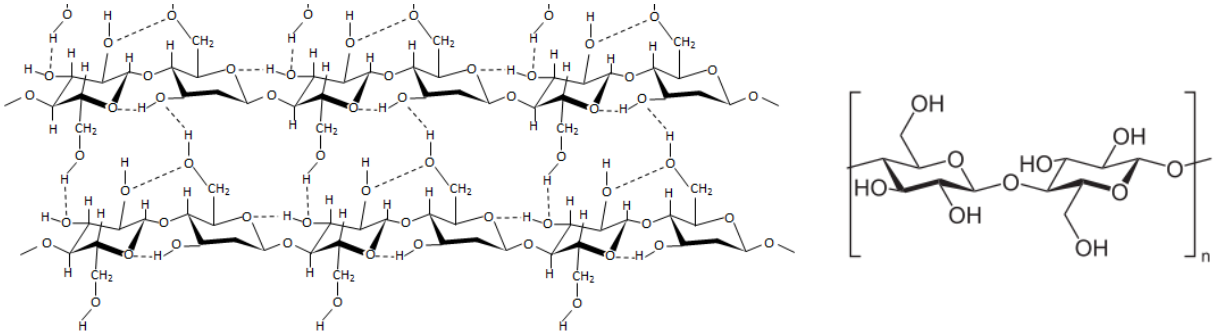

Figure 3: BC network (left) with a close-up of the BC molecular structure [11]

4. Justification

Current work being done in the Singer Research Group with found that liquid crystal-infiltrated BC mats behave similarly to polymer-dispersed liquid crystals (PDLCs) with respect to dynamic switching. PDLCs are polymers that confine microdroplets of liquid crystals, confining them in a matrix. PDLCs can be used for micro-blinds, smart windows, and other light control and electro-optic applications [12]. Enhancements in the photorefractive response of PDLCs have been recently explored, which include dopants [13], surface plasmon polaritons [14], and nanoscale photoconductive interlayers [15]. Due to their similar switching capabilities and matrix structures, 5CB-filled BC mats may also behave similarly to PDLCs with regards to photorefraction.

5. Methods and Materials

5.1. Two-Beam Coupling

Two-beam coupling techniques were used in this project to explore the photorefractive properties of the samples. The experimental setup used is shown in Figure 4. Blue diode lasers with wavelengths of 405 nm and 488 nm were used. Two-beam coupling involves the mixing of two coherent, p-polarized beams within a sample to produce a refractive index grating. The non-locality of the grating causes one diffracted beam to interact constructively with its companion beam while the other interacts destructively. As a result, one of the beams is amplified while the other is diminished. A schematic of the beam coupling within the material is shown in Figure 5. Significant diffraction only occurs when the electric field is applied to the sample. When the sample thickness falls into the thin film regime (several microns at most), higher orders of self-diffraction may also may also be observed [9].

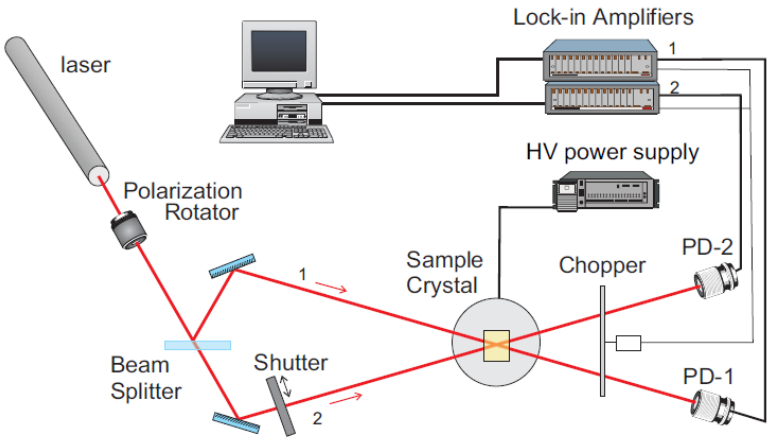

Figure 4: Two-beam coupling experimental setup [4]

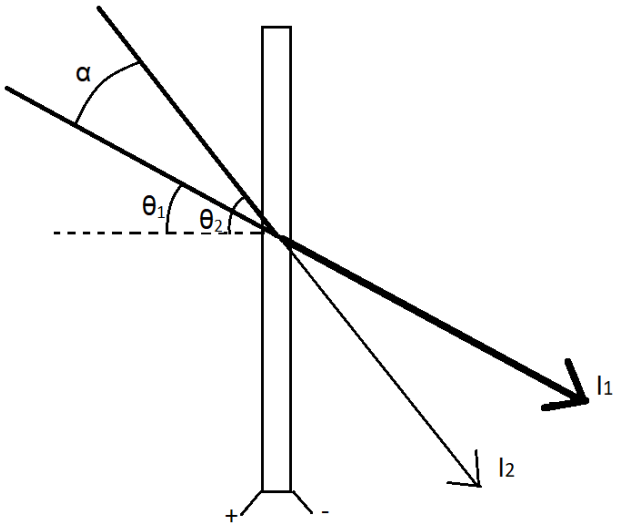

Figure 5: Schematic of beam coupling in the material. I_1 and I_2 are the measured beam intensities, θ_1 and θ_2 are the respective incident angles with respect to normal, and α is the mixing angle. In this case, I_1 is intensified and I_2 is diminished.

In this setup, a laser emits a beam which is then polarized in the p-direction. The beam is split and reflected towards the sample with a mixing angle, α, and the transmitting beams are chopped and measured by two photodetectors. The photodetectors' relative voltages are read by lock-in amplifiers, which are computer-controlled via MATLAB and a GPIB connection. A DC power supply provides the electric field within the sample. In later trials, a function generator and amplifier supply AC electric fields within the sample. Figure 6 shows an example of the data expected to be collected.

The degree of beam coupling is represented by the gain coefficient, $\tilde{\Gamma}$, and is expressed by the following equation

$$\tilde{\Gamma} = -\frac{1}{\tilde{d}} \ln\left[\frac{I_1}{I_2}\right] \quad (1)$$

where I_1 and I_2 are the intensities of the output beams, and $\tilde{d}$ is the effective thickness of the sample, given by the equation

$$\tilde{d} = \frac{d}{\cos\left(\frac{\theta_1+\theta_2}{2}\right)} \qquad (2)$$

where d is the sample thickness, and θ_1 and θ_2 are the incidence angles of the beams [4].

5.2. Samples

There were three different types of samples tested. All three samples had the basic structure as shown in Figure 7, with a slight modification in the BC mat-containing samples. The photorefractive material under investigation will be sandwiched between indium tin oxide (ITO) coated glass substrates that are separated by Mylar spacers. ITO is a transparent conducting material that will serve as the electrodes when an electric field across the sample. The thickness of the cell was determined by the thickness of the Mylar spacers used: 12.5 µm and 25 µm. These thicknesses were confirmed using capacitance measurements and the known dielectric constant [4].

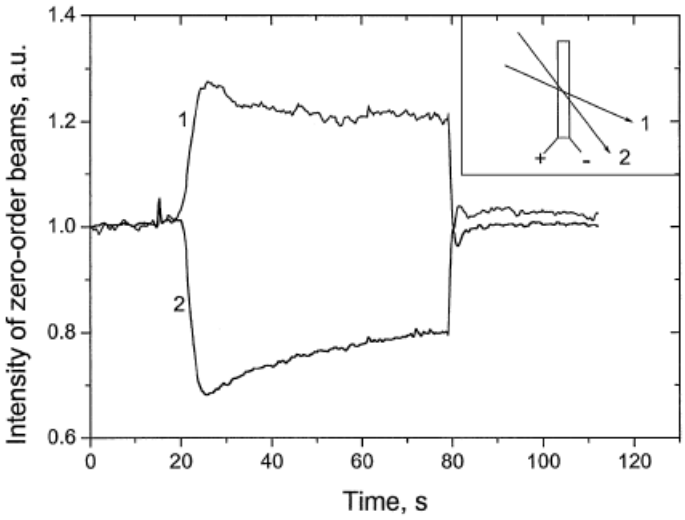

Figure 6: Sample data showing the beam coupling within a sample of homeotropically aligned 5CB. A DC electric field is applied at approximately 20 s and turned off at 80 s [1]

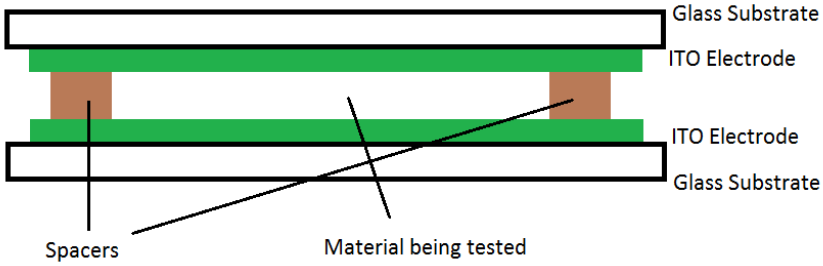

Figure 7: Side-view of a basic test sample

The first kind of sample used for validating the observation of the photorefractive effect contained 5CB in a sandwich cell. The second sample was sandwich cell containing 5CB doped with a fullerene (C_{60}) sensitizer in order to verify that the refractive index grating is confined to the liquid crystal-cell interface [1].

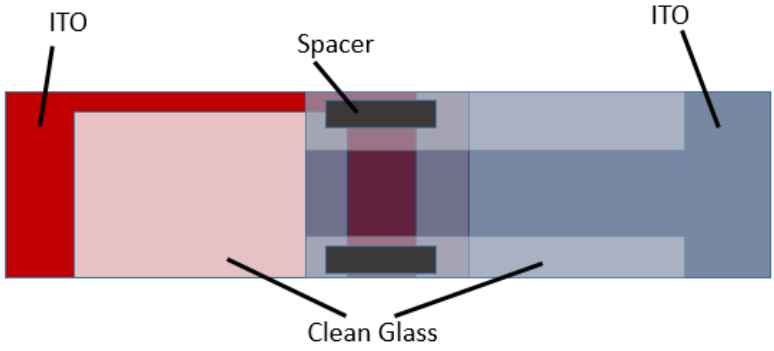

Figure 8: C- and T-shape of the ITO for the BC mat samples with one substrate in red and the other in blue.

The third contained the 5CB-infiltrated BC mat. The ITO for this sample type was etched with hydrochloric acid to form a C- and T- shape as shown in Figure 8. This was done to confine the electric field to the BC mat and prevent electrical shorts across the sample. When no electric field is applied, the material is in a scattering state and appears opaque to the eye. An AC field is necessary to transition the sample to a transparent state. The sample must be in a transparent state while making photorefractive measurements.

5.3. Fabrication

5.3.1. 5CB Cell Sample

For these samples, the sandwich cells were assembled first, then filled via capillary action with liquid crystal. Clean ITO-coated glass was treated with hexadecyl trimethyl ammonium bromide (CTAB) in order to promote homeotropic alignment of the liquid crystal. This was done by drop casting a CTAB solution onto the ITO and vigorously wiping the slides, leaving behind a monolayer. Two slide were pressed together around two Mylar spacers and clamped. The cells were filled with the liquid crystal in the isotropic phase via capillary action at an elevated temperature and sealed with epoxy.

5.3.2. C_{60}-doped 5CB Cell Sample

C_{60} is typically insoluble in 5CB, so in order to create this solution, C_{60} was dissolved in a toluene solution and combined with 5CB. The solvent was then evaporated, and the remaining material was used to fill the cells. The sandwich cells were constructed and filled via capillary action identically to the 5CB cell samples detailed above.

5.3.3. 5CB BC Mat Sample

The BC mat provided by our collaborators had a thickness of 12 µm. The mat was fixed with Kapton tape to an etched ITO slide at the crossing location as shown in Figure 8. Liquid crystal was drop cast onto the mats in the nematic phase at room temperature. The samples were then heated in a vacuum chamber for 24 hours. During this time, the liquid crystal will transition into the isotropic phase and the vacuum will remove voids from the sample. The other etched ITO slide is then placed on top of the filled mat and the sample is encapsulated with epoxy.

Four types of BC mat samples were assembled, as shown in Figure 9. Two of each sample type were fabricated.

Untreated ITO, 5CB-infiltrated mat	Untreated ITO, C_{60}-doped 5CB-infiltrated mat
CTAB-treated ITO, 5CB-infiltrated mat	CTAB-treated ITO, C_{60}-doped 5CB-infiltrated mat

Figure 9: The four varieties of BC mat samples created

5. Results

The alignment of the two beam coupling was confirmed with the successful observation of higher order diffraction using the 5CB cell samples. As seen in Figure 10, the first higher order diffracted beams were observed with the application of a DC voltage. This was observed with a mixing angle of 4.5^o at an incidence angle of 45^o.

Beam coupling was also observed with the 5CB cell samples as well as the C_{60}-doped 5CB cell samples. With p-polarized beams of 7.5 mW mixing at an angle of 4.5^o, significant beam coupling was observed with the application of a DC electric field when at least 3.0 V were applied across the 12.5 µm thick sample. The gain was maximized at an incidence angle of approximately 45^o, and no coupling was observed at normal incidence. An example of collected beam coupling data can be seen in Figure 11.

No voltage 3.5 V DC applied

Figure 10: ±1st order diffracted beams are observed on the right when a DC voltage of 3.5 V is applied across the 5CB cell.

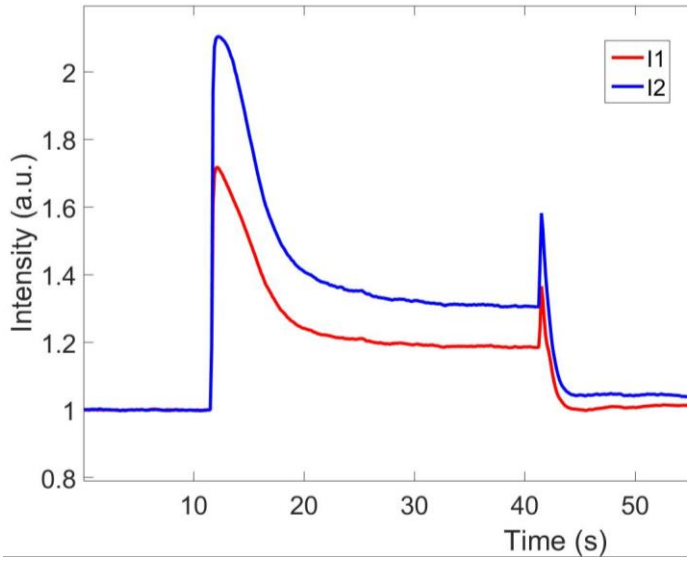

Figure 11: Sample beam coupling data. 3.5 V were applied across a C_{60}-doped 5CB cell sample at 12 s and removed at 41 s. The transients at the beginning and end of the electric field are due to charging and screening [16]

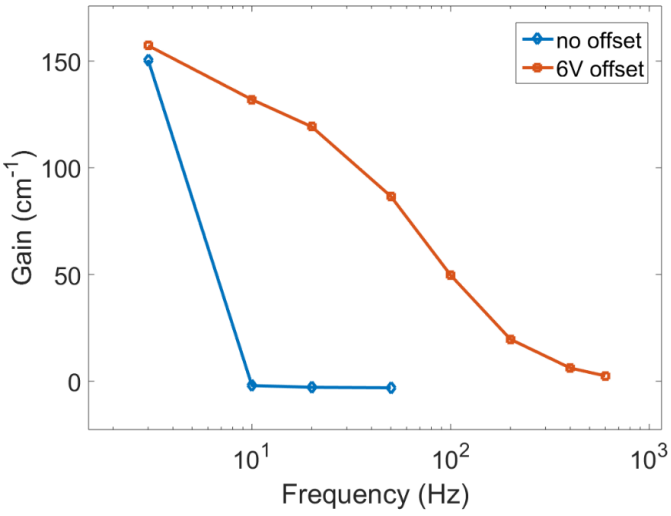

Figure 12: Frequency dependence of gain with the application of 40 V_{pp} across C_{60}-doped 5CB cells.

Beam coupling was also observed in the C_{60}-doped 5CB cells with the application of an AC electric field. Significant gain was observed at low electric field frequencies and decreased as the frequency increased. No gain was observed above 50 Hz. The degree of coupling exhibited an oscillatory behavior at a period much longer than that of the applied field. Though this behavior has been observed in previous studies [17,18], the mechanism behind it is not well understood.

Similar behavior was observed with the application of AC electric fields with a DC offset. However, the addition of a DC offset led to significantly higher gain at a large range of frequencies. While an unbiased AC field did not yield measurable gain at frequencies larger than 50 Hz, samples with an applied AC field with DC bias displayed significant gain that diminished as the frequency approached 600 Hz (Figure 12).

Regarding the BC mat samples, photorefraction has yet to be confirmed. No beam coupling was observed at small mixing angles ($\alpha = 4.5^o$) with the following variables:

- 3 Hz – 10 kHz AC field
- $\theta_2 = 0\text{-}50^o$
- Up to 130 V_{pp}
- Up to 30 mW mixing beams
- Up to 12 V DC offset
- 405 nm and 488 nm beams

Future studies will continue attempting observation of photorefraction with these samples. Another variable to explore is large mixing angles.

7. Conclusion

In summary, dynamic holography methods were used to successfully observe beam coupling in 5CB and C_{60} doped 5CB cells with the application of DC and AC electric fields. DC fields across 5CB and C_{60} doped 5CB cells also yielded higher order diffracted beams. In the C_{60}-doped 5CB cells, an AC electric field with DC offset lead to appreciable gain, a behavior that warrants future exploration.

Though photorefraction has not yet been observed in liquid crystal-infiltrated BC mats, efforts to successfully observe this photorefraction will continue in the future. If successful, future studies will explore how varying the BC mat properties (porosity, thickness, surface treatment, etc.) effects the photorefractive response.

8. Acknowledgements

I would like to thank the Singer Research Group for funding this project, as well as Prof. Ken Singer and Kyle Peters for their guidance. I would also like to thank Ph.D. students Michael McMaster, Bin Liu, and Samuel Schwab for their respective help with the bacterial cellulose samples, PVK samples and optical set-up, and photorefraction.

9. References

[1] Zhang, J., Ostroverkhov, V., Singer, K.D., Reshetnyak, V., Reznikov, Y., 2000. Electrically controlled surface diffraction gratings in nematic liquid crystals. Opt. Lett., OL 25, 414–416.

[2] Indeck, R., Hoang, B., 2012. Organic Electronics. IEEE Emerging Technology Portal.

[3] Zhang, Y., Burzynski, R., Ghosal, S., Casstevens, M.K., 1996. Photorefractive Polymers and Composites. Adv. Mater. 8, 111–125.

[4] Ostroverkhova, O.G., 2001. Nonlinear optical probes and processes in polymers and liquid crystals. Ph.D. Thesis.

[5] Khoo, I.C., 1996. Orientational photorefractive effects in nematic liquid crystal films. IEEE Journal of Quantum Electronics 32, 525–534.

[6] Pepper, D.M., Feinberg, J., Kukhtarev, N.V., 1990. The Photorefractive Effect. Scientific American 263, 62–75.

[7] Collings, P.J., 1990. Liquid Crystals: Nature's Delicate Phase of Matter. Hilger.

[8] Zhang, G., Montemezzani, G., Günter, P., 2000. Orientational photorefractive effect in nematic liquid crystal with externally applied fields. Journal of Applied Physics 88, 1709–1717.

[9] Ren, C.-Y., Shi, H.-X., Ai, Y.-B., Yin, X.-B., Wang, F., Ding, H.-W., 2016. Asymmetric dynamic phase holographic grating in nematic liquid crystal. Chinese Phys. B 25, 094218.

[10] Tercjak, A., Gutierrez, J., Barud, H.S., Ribeiro, S.J.L., 2016. Switchable photoluminescence liquid crystal coated bacterial cellulose films with conductive response. Carbohydr Polym 143, 188–197.

[11] Lustri, W.R., Barud, H.G. de O., Silva Barud, H. da, Peres, M.F.S., Gutierrez, J., Tercjak, A., Junior, O.B. de O., Ribeiro, S.J.L., 2015. Microbial Cellulose — Biosynthesis Mechanisms and Medical Applications. InTech.

[12] Spruce, G., Pringle, R.D., 1992. Polymer dispersed liquid crystal (PDLC) films. Electronics Communication Engineering Journal 4, 91–100.

[13] Li, S., Fu, M., Sun, H., Zhao, Y., Liu, Y., He, D., Wang, Y., 2014. Enhanced Photorefractive and Third-Order Nonlinear Optical Properties of 5CB-Based Polymer-Dispersed Liquid Crystals by Graphene Doping. J. Phys. Chem. C 118, 18015–18020.

[14] Xue, T., Zhao, H., Meng, C., Fu, J., Zhang, J., 2014. Impact of surface plasmon polaritons on photorefractive effect in dye doped liquid crystal cells with ZnSe interlayers. Opt. Express, OE 22, 20964–20972.

[15] Zhao, H., Lian, C., Sun, X., Zhang, J.W., 2011. Nanoscale interlayer that raises response rate in photorefractive liquid crystal polymer composites. Opt. Express, OE 19, 12496–12502.

[16] Korniychuk, P.P., Gabovich, A.M., Singer, K., Voitenko, A.I., Reznikov, Y.A., 2010. Transient and steady electric currents through a liquid crystal cell. Liquid Crystals 37, 1171–1181.

[17] Sun, X., Pei, Y., Yao, F., Zhang, J., Hou, C., 2007. AC electric field assisted orientational photorefractive effect in C 60 -doped nematic liquid crystal. J. Phys. D: Appl. Phys. 40, 3348.

[18] Song, L., Lee, W.-K., Wang, X., 2006. AC electric field assisted photo-induced high efficiency orientational diffractive grating in nematic liquid crystals. Opt. Express, OE 14, 2197–2202.

10. Appendix

i. Problem statement

The existing Matlab function collects data from the experimental setup and plots them after the data collection period finished. This input for this function is the number of data points. This is unfavorable because the runtime of the experiment is not obvious from the number of data points, and the data cannot be seen until the experiment is completed. Therefore, a new function to visualize data in real time must be written. The input for this function should be the runtime of the experiment rather than the number of data points.

ii. Constraints

- The relevant beam intensity data must be plotted in real time with respect to time
- Beam intensities are displayed as volts, as measured by the lock-in amplifiers
- The time is in seconds

iii. Approaches

Two different approaches were attempted. The first involves a script that runs in a loop, continuously collecting data and timestamps, until the user enters a keystroke. The second involves a function with the runtime of the experiment as the input variable. For this length of time, data is collected at specific time intervals.

iv. Analysis

I opted for the second approach listed above because it was the first to be completed and functional. I used the existing function as the foundation for this new version. I wrote the new function in steps, some of which include:

- Connecting the computer to the lock-in amplifiers
- Building arrays using data collected from the lock-in amplifiers
- Plotting the relevant data
- Writing a loop with a length determined by a time input

v. Iterations

The steps I took to write the function are listed above. However, the step that required the most work was to write the actual loop. First, I tried running the loop continuously for the input length of time. Due to the frequency at which the data was collected, this yielded unnecessarily large data files. The second approach I took involved collecting the data at specific time intervals. The time steps for this went through several iterations to optimize the resolution of the data while maintaining a manageable file size.

vi. Standards

Matlab is used by the Singer Research Group to collect and analyze data in the optics lab. GPIB connections link the apparatus to the computer.